Eur. Phys. J. C (2014) 74:2738
DOI 10.1140/epjc/s10052-014-2738-1

THE EUROPEAN PHYSICAL JOURNAL C

Regular Article - Theoretical Physics

Warm anisotropic inflationary universe model

M. Sharif[a], **Rabia Saleem**[b]

Department of Mathematics, University of the Punjab, Quaid-e-Azam Campus, Lahore 54590, Pakistan

Received: 22 November 2013 / Accepted: 3 January 2014 / Published online: 1 February 2014

Abstract This paper is devoted to the study of warm inflation using vector fields in the background of a locally rotationally symmetric Bianchi type I model of the universe. We formulate the field equations, and slow-roll and perturbation parameters (scalar and tensor power spectra as well as their spectral indices) in the slow-roll approximation. We evaluate all these parameters in terms of the directional Hubble parameter during the intermediate and logamediate inflationary regimes by taking the dissipation factor as a function of the scalar field as well as a constant. In each case, we calculate the observational parameter of interest, i.e., the tensor–scalar ratio in terms of the inflaton. The graphical behavior of these parameters shows that the anisotropic model is also compatible with WMAP7 and the Planck observational data.

1 Introduction

In the context of cosmology, it has become an undeniable fact through the combined efforts of type Ia supernova, the large scale structure (LSS), cosmic microwave background (CMB), and WMAP studies that the universe is undergoing a stage of accelerating expansion [1–7]. This cosmic behavior might be due to the repulsive nature of a missing energy (due to the large negative pressure) called dark energy (DE), which occupies 70 percent of the universe. It is described by a tiny time-independent cosmological constant (Λ) obeying $\omega = -1$ (ω is the equation of state (EoS) parameter). Due to the fine-tuning and cosmic coincidence issues [8] of this constant, the search for a variety of DE models is ongoing. The dynamical nature of DE is divided into two categories: scalar field models (quintessence, phantom with negative kinetic term, k-essence, quintom (unification of quintessence and phantom) etc.) [9–14] and interacting DE models (Chaplygin gas having novel EoS, holographic DE, Ricci DE etc.) [15–18].

The standard cosmology (big-bang model) successfully explains the observations of CMB radiation, but still there are some unresolved issues. The early universe is facing some long standing problems including the horizon problem (why is the universe isotropic and homogeneous on large scale structure?), flatness (why is $\Omega_{\text{total}} \approx 1$ today?), the monopole issue (why do not they exist?); and finally we may ask: what is the origin of the fluctuations? See Refs. [19–22]. The inflationary scenario ($\omega < -\frac{1}{3}$) proved to be a cornerstone to explain the mechanism of the early universe and provides the most compelling solution of these problems. The constant Λ can also resolve these issues but unfortunately, in this case inflation never ends and the normal evolution of the cosmos remains impossible.

A scalar field (composed of kinetic and potential terms coupled to gravity) is the perfect candidate to produce the dynamical framework and act as a source for inflation. In field theory, a spin zero particle is usually defined by a scalar field, whereas, mathematically, it is a function of space and time. It has the ability to interpret the distribution of LSS and the observed anisotropy of the CMB radiation elegantly in the inflationary era [23–25]. Golovnev et al. [26] discussed the vector inflation models based on an orthogonal triplet, non-minimally coupled to gravity, which shows a similar behavior as the scalar fields in a flat universe. It has been proved that many cosmological models characterized by vectors non-minimally coupled to the curvature, such as vector inflation, contain ghosts. Ghosts are associated with the longitudinal vector polarization present in these models, and they are found from studying the sign of eigenvalues of the kinetic matrix for the physical perturbations. They introduce two main problems: firstly, they make the theories ill defined at the quantum level in the high energy regime; secondly, they create an instability already at the linearized level. This happens because the eigenvalue corresponding to the ghost crosses zero during the cosmological evolution [27].

[a] e-mail: msharif.math@pu.edu.pk

[b] e-mail: rabiasaleem1988@yahoo.com

The inflation regime is divided into two parts, i.e., slow-roll and reheating epochs. During the slow-roll period, the universe inflates as the interactions between scalar fields (inflatons) and other fields become meaningless and the potential energy dominates the kinetic term [28–30]. Reheating is the end stage of inflation; here the kinetic and potential energies are comparable and the inflaton starts to oscillate around the minimum of its potential [31]. Warm inflation [32,33] has the attractive feature of joining the expanding universe with the end of vector inflation. This motivated researchers to discuss the inflationary scenario in the context of warm inflation. During this regime, the dissipation effects become strong enough due to the production of thermal fluctuations of the constant density which play a vital role in the formation of initial fluctuations necessary for LSS construction. An additional advantage of warm vector inflation is that the universe stops inflating and smoothly enters into the radiation-dominated phase [34–36].

Inflation is usually discussed in the context of intermediate and logamediate scenarios. Intermediate inflation is motivated by string or M theory and proved to be the exact solution of the inflationary cosmology containing a particular form of the scale factor [37]. By adding the higher order curvature correction (which is proportional to the Gauss–Bonnet (GB) term) to the Einstein–Hilbert action, one obtains a ghost-free action. Gauss–Bonnet interaction is the leading order in the expansion of the inverse string tension, 'α', of the low-energy string effective action [38,39]. This theory may be applied to BH solutions [40], acceleration of the late time universe [41,42], and initial singularity problems [43]. The 4-dimensional GB interaction with dynamical dilatonic scalar coupling leads to an intermediate form of the scale factor [37].

In the intermediate era, the universe expands at a rate slower than the standard de Sitter inflation ($a = a_0 \exp(H_0 t)$; $a_0,\ H_0 > 0$) but faster than power-law inflation ($a = t^m,\ m > 1$) [44]. On the other hand, the logamediate inflation [45] is motivated by applying weak general conditions on the indefinitely expanding cosmological models. Barrow [46] applied this scenario to constant, power-law, and exponential types of scalar field. The effective potential and various types of potential associated with this model are used in different DE models and in supergravity, Kaluza–Klein as well as string theories, respectively [5,47,48]. It has been proved that the power spectrum is red or blue tilted for this type of inflation. Setare and Kamali [49] discussed this issue of warm inflation using gauge fields in intermediate as well as logamediate scenarios. Warm inflation is also studied in generalized teleparallel gravity [50].

In a recent paper [51], Setare and Kamali have discussed warm vector inflation in intermediate and logamediate scenarios for the FRW model and proved the physical compatibility of these results with WMAP7 data [5,47,48] through the perturbed parameters. In this paper, we study the above mentioned scenario in the framework of the anisotropic model of the universe, i.e., in the locally rotationally symmetric (LRS) Bianchi I (BI) framework. The format of the paper is as follows. In the next section, we construct the field equations from the action and calculate the corresponding pressure as well as the energy density, imposing the slow-roll condition. We also formulate the slow-roll as well as scalar and tensor perturbed parameters. In Sect. 3, we evaluate the Hubble parameter, scalar field as well as slow-roll and perturbed parameters in two regimes:

(1) intermediate inflation, and

(2) logamediate inflation. The inflationary universe is further studied with a variable and a constant dissipation factor. The results are summarized in Sect. 4.

2 Basic formalism and perturbations

In this section, we briefly discuss the inflationary model using the anisotropic background of the universe. A massive vector field, non-minimally coupled to gravity, is presented by the following action [26]:

$$\mathcal{S}=-\frac{1}{2}\int \mathrm{d}^4x\sqrt{-g}\left(R+\frac{1}{2}F_{\alpha\beta}F^{\alpha\beta}-\frac{R}{6}A^\alpha A_\alpha-V(A^\alpha A_\alpha)\right),$$

where $\alpha, \beta = 0, 1, 2, 3$, the field strength ($F_{\alpha\beta}$) and potential ($V$) are defined as follows:

$$F_{\alpha\beta} = \partial_\alpha A_\beta - \partial_\beta A_\alpha, \quad V(A^\alpha A_\alpha) = m^2 A^\alpha A_\alpha + \cdots$$

This non-minimal coupling of the vector field has an opposite effect, i.e., it violates the conformal invariance of the massless vector field and forces it to behave just like a minimally coupled scalar field. The variation of the action with respect to A_α yields the following equations of motion:

$$\frac{1}{\sqrt{-g}}\partial_\alpha(\sqrt{-g}F^{\alpha\beta})+\frac{R}{6}A^\beta+\frac{\partial V}{\partial A_\beta}=0, \tag{1}$$

where $\partial_\alpha = \frac{\partial}{\partial x^\alpha}$. An isotropic model (FRW) is unsteady near the initial singularity and thus unable to explain the early mechanism of the universe. One needs an appropriate geometry, which is more concise and general than the isotropic and homogeneous FRW universe. Bianchi models are prime and viable models to discuss the behavior of the early universe. A BI model, being the straightforward generalization of the flat FRW model, is one of the simplest models of the anisotropic universe.

The line element for the LRS BI model ($b(t) = c(t)$) is given as

$$\mathrm{d}s^2 = -\mathrm{d}t^2 + a^2(t)\mathrm{d}x^2 + b^2(t)(\mathrm{d}y^2 + \mathrm{d}z^2),$$

where $a(t)$, $b(t)$ are the scale factors along x-axis and (y, z)-axis, respectively. This metric can be transformed into the following form using a linear relationship, $a = b^n$, $n \neq 1$ [52,53]:

$$ds^2 = -dt^2 + b^{2n}(t)dx^2 + b^2(t)(dy^2 + dz^2). \quad (2)$$

In this scenario, Eq. (1) leads to

$$\ddot{A}_i + \left(\frac{n+2}{3}\right) b^{\frac{(n-4)}{3}} \dot{b}(\dot{A}_i - \partial_i A_0) + \frac{1}{b^{\frac{2(n+2)}{3}}}(\partial_i(\partial_k A_k) - \Delta A_i) - \partial_i \dot{A}_0 + \left(m^2 + \frac{R}{6}\right) A_i = 0,$$

$$-b^{-\frac{2(n+2)}{3}} \Delta A_0 + \left(m^2 + \frac{R}{6}\right) A_0 + b^{-\frac{2(n+2)}{3}} \partial_i \dot{A}_i = 0, \quad (3)$$

where a dot represents the time rate of change. Applying the condition of the homogeneous vector field, i.e., $\partial_i A_\alpha = 0$ to Eq. (3), one deduces $A_0 = 0$. Another variable, $\mathcal{B}_i = \frac{A_i}{b^{\frac{n+2}{3}}}$, is introduced for the scalar field in place of A_i. Consequently, Eq. (3) has a similar form to the massive minimally coupled scalar field, which can be written as

$$\ddot{\mathcal{B}}_i + (n+2)H_2\dot{\mathcal{B}}_i + V'(\mathcal{B}_j\mathcal{B}^j)\mathcal{B}_i = 0,$$

or equivalently

$$\ddot{\mathcal{B}}_i + (n+2)H_2\dot{\mathcal{B}}_i + m^2\mathcal{B}_i = 0, \quad (4)$$

where $H_2 = \frac{\dot{b}}{b}$ is the directional Hubble parameter, and the prime denotes a derivative with respect to $\mathcal{B}_j\mathcal{B}^j$.

The corresponding energy-momentum tensor can be obtained by varying the action with respect to the metric $(g^{\alpha\beta})$ [26]. The temporal and the spatial components of the energy-momentum tensor are

$$\begin{aligned} T_0^0 &= \frac{1}{2}(\dot{\mathcal{B}}_k^2 + V(\mathcal{B}^i\mathcal{B}_i)), \\ T_j^i &= \left[-\frac{5}{6}\dot{\mathcal{B}}_k^2 + \frac{1}{2}V(\mathcal{B}^2) - \frac{2}{3}\left(\frac{n+2}{3}\right)H_2\dot{\mathcal{B}}_k\mathcal{B}_k \right. \\ &\quad \left. -\frac{1}{3}\left(\left(\frac{n+2}{3}\right)\dot{H}_2 + 3\left(\frac{n+2}{3}\right)^2 H_2^2 - V'(\mathcal{B}^2)\right)\mathcal{B}_k^2\right] \\ &\quad \times\delta_j^i + \dot{\mathcal{B}}_i\dot{\mathcal{B}}_j + \left(\frac{n+2}{3}\right)H_2(\dot{\mathcal{B}}_i\mathcal{B}_j + \dot{\mathcal{B}}_j\mathcal{B}_i) \\ &\quad + \left(\left(\frac{n+2}{3}\right)\dot{H}_2 + 3\left(\frac{n+2}{3}\right)^2 H_2^2 - V'(\mathcal{B}^2)\right)\mathcal{B}_i\mathcal{B}_j, \end{aligned} \quad (5)$$

where k stands for the summation index and $\mathcal{B}_k$ satisfies Eq. (4) for any vector field. We have considered the LRS BI model of the universe with a homogeneous vector field, which does not contain the off-diagonal terms in the energy-momentum tensor. In order to make the spatial component of the energy-momentum tensor diagonal, we use various fields simultaneously. Therefore, a triplet of the mutually orthogonal vector fields is defined as follows [54]:

$$\sum_a \mathcal{B}_i^a\mathcal{B}_j^a = |\mathcal{B}|^2\delta_i^j.$$

Using the above conditions with an ansatz, $\mathcal{B}_i^a = |\mathcal{B}|\delta_i^a$ in Eq. (5), the components of the energy-momentum tensor reduce to diagonal form, thus

$$\begin{aligned} T_0^0 &= \rho_v = \frac{3}{2}(\dot{\mathcal{B}}_k^2 + V(|\mathcal{B}|^2)), \\ T_j^i &= -P_v\delta_j^i = -\frac{3}{2}(\dot{\mathcal{B}}_k^2 - V(|\mathcal{B}|^2))\delta_j^i. \end{aligned}$$

These equations are similar to the equations which are evaluated in [55] for a massive scalar field. The choice of $|\mathcal{B}| > 1$ corresponds to the inflation epoch in the slow-roll limit $(\dot{\mathcal{B}}_k^2 \ll V(\mathcal{B}^2))$ for which $\rho_v = -P_v$.

We assume that the total energy density of the universe is the sum of energy density of the vector field (ρ_v) and radiation (ρ_γ). The mechanism of warm vector inflation can be represented by the first field equation (evolution equation) and the conservation equations given as

$$\begin{aligned} H_2^2 &= \frac{1}{1+2n}\left(\frac{3}{2}(\dot{\mathcal{B}}_k^2 + V(|\mathcal{B}|^2)) + \rho_\gamma\right) = \frac{1}{1+2n}(\rho_v + \rho_\gamma), \\ \dot{\rho}_v &+ (n+2)H_2(\rho_v + P_v) = -\eta\dot{\mathcal{B}}^2, \\ \dot{\rho}_\gamma &+ \frac{4(n+2)}{3}H_2\rho_\gamma = \eta\dot{\mathcal{B}}^2, \end{aligned} \quad (6)$$

where η, T_γ stand for the dissipation or friction factor and the temperature of the thermal bath, respectively. We assume a suitable form of $\eta = \eta_0\frac{T_\gamma^3}{\mathcal{B}^2}$, where η_0 is any constant and T_γ can be extracted via quantum field theory methods which hold for low temperatures [56,57]. In this method, the inflaton interacts with the heavy intermediate field (which acts as a catalyst) which could decay into a massless field called radiation. Here η is taken to be positive (by the second law of thermodynamics) which implies that the energy density of the scalar field decays into radiation density. During the inflation era, $\rho_v \sim V(A^2)$, and the energy density of the inflaton exceeds the radiation density $(\rho_v > \rho_\gamma)$. Further, we apply two limits on the above dynamic equations, i.e., the slow-roll approximation $(\ddot{\mathcal{B}} \ll ((n+2)H_2 + \frac{\eta}{3})\dot{\mathcal{B}})$, and quasi-stability of the radiation production where $\dot{\rho}_\gamma \ll 4(\frac{n+2}{3})H_2\rho_\gamma$, $\dot{\rho}_\gamma \ll \eta\dot{\mathcal{B}}^2$ [32,33]. Using all these conditions, we can write Eq. (6) as follows:

$$-\frac{1}{2}V' = (n+2)\left(1 + \frac{\chi}{3}\right)H_2\dot{\mathcal{B}}, \quad (7)$$

$$\rho_\gamma = \frac{3}{4}\chi\dot{\mathcal{B}}^2 = \frac{(1+2n)}{8(n+2)^2}\frac{\chi}{(1+\frac{\chi}{3})^2}\frac{V'^2}{V} = C_\gamma T_\gamma^4, \quad (8)$$

$$H_2^2 = \frac{3}{2(1+2n)}V, \quad (9)$$

where $\chi = \frac{\eta}{(n+2)} H_2$ denotes the rate of dissipation, where we distinguish the strong ($\chi > 1$) and weak ($\chi < 1$) dissipation regions. The radiation energy density is also written in the form $C_\gamma T_\gamma^4$, where $C_\gamma = \frac{\pi^2 g_*}{30}$ and g_* is known as the number of relativistic degrees of freedom. Using Eqs. (7) and (9) in (8), the temperature of the thermal bath can be obtained as follows:

$$T_\gamma = \left[\frac{-(1+2n)\chi \dot{H}_2}{2C_\gamma (n+2)(1+\frac{\chi}{3})}\right]^{\frac{1}{4}}. \tag{10}$$

The dimensionless slow-roll parameters (ϵ, λ) [58] of the warm vector inflation can be calculated using Eq. (9) as

$$\epsilon = -\frac{3}{(n+2)H_2}\frac{\mathrm{d}}{\mathrm{d}t}\left(\ln\left(\frac{n+2}{3}H_2\right)\right) = -\frac{3}{(n+2)}\frac{\dot{H}_2}{H_2^2} = \frac{1+2n}{2(n+2)^2(1+\frac{\chi}{3})}\frac{V'^2}{V^2}, \tag{11}$$

$$\lambda = -\frac{3}{(n+2)}\frac{\ddot{H}_2}{H_2\dot{H}_2} = 2\epsilon - \frac{3\dot{\epsilon}}{(n+2)H_2\epsilon} = 2\epsilon + \frac{6(1+2n)}{(n+2)^2(3+\chi)}\left(\frac{V'}{V}\right)\left[\frac{V''}{V'} - \frac{V''}{V} - \frac{3}{2}\frac{\chi'}{(3+\chi)}\right]. \tag{12}$$

The energy density of the scalar field can be expressed in terms of the radiation density using Eqs. (9) and (11) as

$$\rho_\gamma = \frac{1}{2}\left(\frac{\chi}{3+\chi}\right)\epsilon\rho_v.$$

Here, we consider the strong dissipative regime where $\chi \gg 1$, which implies that $\eta \gg 3(n+2)H_2$. Consequently, ρ_γ can be simplified to

$$\rho_\gamma = \frac{1}{2}\epsilon\rho_v. \tag{13}$$

The condition of the warm inflation epoch, i.e., $\rho_v > 2\rho_\gamma$, can be verified via the inequality $0 < \ddot{b} < 1$ for which $\epsilon < 1$. This inflationary scenario ends at $\epsilon = 1$ where the inflaton energy density becomes twice the radiation density. The number of e-folds at the two different cosmological times t (beginning of inflation) and t_1 (end of inflation) is defined as follows:

$$N = \frac{(n+2)}{3}\int_t^{t_1} H_2 \mathrm{d}t = -\frac{(n+2)^2}{2(1+2n)}\int_t^{t_1}(3+\chi)\frac{V}{V'}\mathrm{d}t. \tag{14}$$

Now we evaluate the scalar and tensor perturbations for the anisotropic LRS BI model of the universe in the case of small scale structures by varying the field $\mathcal{B}$. In non-warm and warm inflation, quantum and thermal fluctuations, respectively, yield [59–62]

$$\langle\delta\mathcal{B}\rangle_{\text{quantum}} = \left(\frac{n+2}{3}\right)^2\frac{H_2^2}{2\pi},$$
$$\langle\delta\mathcal{B}\rangle_{\text{thermal}} = \left(\frac{n+2}{3(4\pi)^3}\right)^{\frac{1}{4}}(\eta H_2 T_\gamma^2)^{\frac{1}{4}}. \tag{15}$$

In cosmology, a useful function of the wave number (k), known as power spectrum, is introduced to quantify the variance in the fluctuations due to the inflaton. In a warm inflationary universe, the scalar power spectrum is given by [63]

$$\Delta_R^2(k) = \left(\frac{n+2}{3}\right)^2\left(\frac{H_2}{\dot{\mathcal{B}}}\langle\delta\mathcal{B}\rangle_{\text{thermal}}\right)^2. \tag{16}$$

Using Eqs. (6), (9), and (15), we can calculate the power spectrum of scalar perturbation in the form

$$\Delta_R^2(k) = -\left[\frac{(n+2)^5\eta^3 T_\gamma^2}{972(1+2n)^2(4\pi)^3}\right]^{\frac{1}{2}}\frac{H_2^{\frac{3}{2}}}{\dot{H}_2} = \left[\frac{(n+2)^5\eta^5 T_\gamma^2}{6^{\frac{3}{2}}972(1+2n)^{\frac{5}{2}}(4\pi)^3}\right]^{\frac{1}{2}}\frac{V^{\frac{5}{4}}}{V'^2}. \tag{17}$$

The second important parameter to study the fluctuations is the scalar spectral index (n_s). For the present model, it is defined as

$$n_s - 1 = -\frac{\mathrm{d}\ln\Delta_R^2(k)}{\mathrm{d}\ln k}. \tag{18}$$

The tensor perturbation ($\Delta_T^2(k)$) and its spectral index (n_T) for the anisotropic universe are

$$\Delta_T^2(k) = \left(\frac{n+2}{3\pi}\right)^2 H_2^2 = \left(\frac{(n+2)^2}{3(1+2n)}\right)\frac{V}{\pi^2}, \tag{19}$$

$$n_T = -2\epsilon. \tag{20}$$

The tensor–scalar ratio (R) has the following form:

$$R = -\left[\frac{48(1+2n)(4\pi)^3}{(n+2)\pi^4\eta^3 T_\gamma^2}\right]^{\frac{1}{2}} H_2^{\frac{1}{2}}\dot{H}_2. \tag{21}$$

According to the observations of WMAP+BAO+SN, the perturbed scalar power spectrum is constrained to $\Delta_R^2(k_0 = 0.002 Mpc^{-1}) = (2.445 \pm 0.096) \times 10^{-9}$ [23–25]. In this context, the physically acceptable range of the tensor–scalar ratio is determined, i.e., by $R < 0.22$, representing the expanding universe.

3 Intermediate and logamediate inflation

In this section, we discuss the warm vector inflation in the context of intermediate and logamediate inflation by treating η as a function of $\mathcal{B}$ as well as a constant.

3.1 Intermediate inflation

In theintermediate scenario, the scale factor follows the law [37]

$$b(t) = b_0 \exp(\mu t^g), \quad \mu > 0,\ 0 < g < 1. \tag{22}$$

The number of e-folds for this model can be calculated using Eq. (14) as

$$N = \frac{(n+2)}{3}\mu(t^g - t_1^g). \tag{23}$$

Firstly, we explore the dynamics of warm intermediate inflation by considering the variable dissipation factor.

3.1.1 Case 1: $\eta = \eta_0 \frac{T_\gamma^3}{\mathcal{B}^2}$, $\eta_0 = constant$

Here, we evaluate some quantities which are useful to determine the parameters defined in the previous section. The scalar potential is evaluated in terms of cosmic time t using Eq. (9) as

$$V = \frac{2(1+2n)}{3}(\mu g)^2 t^{2(g-1)}. \tag{24}$$

The scalar field and the directional Hubble parameter are found using Eqs. (7), (9), (10), and (24) as follows:

$$\mathcal{B} = \mathcal{B}_0 \exp(\omega_0 t^{\frac{5g+2}{8}}), \quad H_2 = \mu g \left(\frac{\ln\mathcal{B} - \ln\mathcal{B}_0}{\omega_0}\right)^{\frac{8(g-1)}{5g+2}}, \tag{25}$$

where $\omega_0 = [\frac{2}{3\eta_0}(\frac{1+2n}{n+2})^{\frac{1}{4}}(\frac{2C_\gamma}{3})^{\frac{3}{4}}]^{\frac{1}{2}}\frac{(1-g)^{\frac{1}{8}}(\mu g)^{\frac{5}{8}}}{5g+2}$ is a pure constant. In this context, the slow-roll parameters take the form

$$\epsilon = \left(\frac{3}{n+2}\right)\frac{1-g}{\mu g}\left(\frac{\ln\mathcal{B} - \ln\mathcal{B}_0}{\omega_0}\right)^{\frac{-8g}{5g+2}},$$
$$\lambda = \left(\frac{3}{n+2}\right)\frac{2-g}{\mu g}\left(\frac{\ln\mathcal{B} - \ln\mathcal{B}_0}{\omega_0}\right)^{\frac{-8g}{5g+2}}. \tag{26}$$

The radiation density (13) can be calculated in terms of the scalar field as

$$\rho_\gamma = \frac{3(1+2n)}{2}\epsilon H_2^2 = \frac{9(1+2n)}{2(n+2)}(\mu g)(1-g)\left(\frac{\ln\mathcal{B} - \ln\mathcal{B}_0}{\omega_0}\right)^{\frac{8(g-2)}{5g+2}}. \tag{27}$$

The inflationary era ($\epsilon < 1$) has the scalar field of magnitude, $\mathcal{B}$.

We assume that $\mathcal{B}_1$ is another field, which is produced at the end of inflation and could be found by fixing $\epsilon = 1$ as

$$\mathcal{B}_1 = \mathcal{B}_0 \exp\left[\omega_0\left(\frac{3(1-g)}{(m+2)\mu g}\right)^{\frac{5g+2}{8g}}\right].$$

Inserting the values of the two different cosmic times (using $\mathcal{B}$ and $\mathcal{B}_1$) in Eq. (23), we get

$$N = \left(\frac{n+2}{3}\right)\mu\left[\left(\frac{\ln\mathcal{B} - \ln\mathcal{B}_0}{\omega_0}\right)^{\frac{8(g-2)}{5g+2}} - \left(\frac{\ln\mathcal{B}_1 - \ln\mathcal{B}_0}{\omega_0}\right)^{\frac{8(g-2)}{5g+2}}\right].$$

These two equations yield $\mathcal{B}$ in terms of N in the following form:

$$\mathcal{B} = \mathcal{B}_0 \exp\left[\omega_0\left(\left(\frac{3}{n+2}\right)\left(\frac{N}{\mu} + \frac{1-g}{g\mu}\right)\right)^{\frac{5g+2}{8g}}\right]. \tag{28}$$

Using Eqs. (10) and (25) in (17), the perturbed scalar power spectrum in warm vector intermediate inflation [which can also be expressed in terms of e-folds with the help of Eq. (28)] is

$$\begin{aligned}\Delta_R^2(k) &= \left(\frac{\eta_0^3}{972(4\pi)^3}\right)^{\frac{1}{2}}\left[\frac{3^{11}(n+2)^{29}(\mu g)^{15}(1-g)^3}{(2C_\gamma)^{11}(1+2n)^5}\right]^{\frac{1}{8}}\mathcal{B}^{-3} \\ &\quad\times\left(\frac{\ln\mathcal{B} - \ln\mathcal{B}_0}{\omega_0}\right)^{\frac{15g-18}{5g+2}} \\ &= \left(\frac{\eta_0^3}{972(4\pi)^3}\right)^{\frac{1}{2}}\left[\frac{3^{11}(n+2)^{29}(\mu g)^{15}(1-g)^3}{(2C_\gamma)^{11}(1+2n)^5}\right]^{\frac{1}{8}}\mathcal{B}_0^{-3} \\ &\quad\times\exp\left[-3\omega_0\left(\left(\frac{3}{m+2}\right)\left(\frac{N}{\mu} + \frac{1-g}{g\mu}\right)\right)^{\frac{5g+2}{8g}}\right] \\ &\quad\times\left[\left(\frac{3}{n+2}\right)\left(\frac{N}{\mu} + \frac{1-g}{g\mu}\right)\right]^{\frac{15g-18}{8g}}.\end{aligned}$$

Using this equation in the scalar spectral index (18), we have

$$\begin{aligned}n_s &= 1 + \left(\frac{3}{n+2}\right)\left(\frac{15g-18}{8g\mu}\right)\left(\frac{\ln\mathcal{B} - \ln\mathcal{B}_0}{\omega_0}\right)^{\frac{-8g}{5g+2}} \\ &= 1 + \left(\frac{3}{n+2}\right)\left(\frac{15g-18}{8g\mu}\right)\left[\left(\frac{3}{n+2}\right)\left(\frac{N}{\mu} + \frac{1-g}{g\mu}\right)\right]^{-1}.\end{aligned} \tag{29}$$

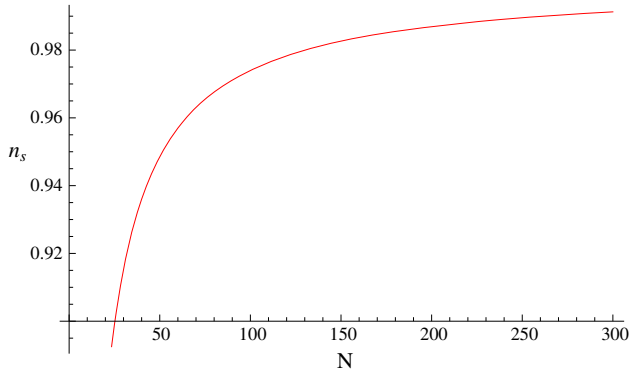

Fig. 1 The graph of n_s versus number of e-folds for $\mu = 1,\ g = \frac{1}{2},\ n \approx 0.5$ in the intermediate scenario

Figure 1 shows the increasing behavior of n_s with respect to N. The observational value of $n_s = 0.96$ corresponds to $N = 60$, which indicates the physical compatibility of this anisotropic model with WMAP7 data. Equations (19) and (20) give the tensor power spectrum as well as the spectral index, respectively, as follows:

$$\Delta_T^2(k) = \frac{2}{9\pi^2}(n+2)^2(\mu g)^2\left(\frac{\ln\mathcal{B}-\ln\mathcal{B}_0}{\omega_0}\right)^{\frac{16(g-1)}{5g+2}} = \frac{2}{9\pi^2}(n+2)^2(\mu g)^2\left[\left(\frac{3}{n+2}\right)\left(\frac{N}{\mu}+\frac{1-g}{g\mu}\right)\right]^{\frac{2(g-1)}{g}},$$

$$n_T = -2\left(\frac{3}{n+2}\right)\left(\frac{1-g}{\mu g}\right)\left(\frac{\ln\mathcal{B}-\ln\mathcal{B}_0}{\omega_0}\right)^{\frac{-8g}{5g+2}} = -\frac{6(1-g)}{(n+2)\mu g}\left[\left(\frac{3}{m+2}\right)\left(\frac{N}{\mu}+\frac{1-g}{g\mu}\right)\right]^{-1}.$$

The tensor–scalar ratio is obtained as

$$R = \left(\frac{48(4\pi)^3(n+2)^4(\mu g)^4}{\pi^4\eta_0^3}\right)^{\frac{1}{2}} \times\left[\frac{(2C_\gamma)^{11}(1+2n)^5}{3^{11}(n+2)^{29}(\mu g)^{15}(1-g)^3}\right]^{\frac{1}{8}} \times\mathcal{B}^{-3}\left(\frac{\ln\mathcal{B}-\ln\mathcal{B}_0}{\omega_0}\right)^{\frac{g+2}{5g+2}} = \left(\frac{48(4\pi)^3(n+2)^4(\mu g)^4}{\pi^4\eta_0^3}\right)^{\frac{1}{2}} \times\left[\frac{(2C_\gamma)^{11}(1+2n)^5}{3^{11}(n+2)^{29}(\mu g)^{15}(1-g)^3}\right]^{\frac{1}{8}}\mathcal{B}_0^3 \times\exp\left[3\omega_0\left(\left(\frac{3}{n+2}\right)\left(\frac{N}{\mu}+\frac{1-g}{g\mu}\right)\right)^{\frac{5g+2}{8g}}\right] \times\left[\left(\frac{3}{n+2}\right)\left(\frac{N}{\mu}+\frac{1-g}{g\mu}\right)\right]^{\frac{g+2}{8g}}.$$

Rewriting the above equation in the form of n_s, we have

$$R = \left(\frac{48(4\pi)^3(n+2)^4(\mu g)^4}{\pi^4\eta_0^3}\right)^{\frac{1}{2}} \times\left[\frac{(2C_\gamma)^{11}(1+2n)^5}{3^{11}(n+2)^{29}(\mu g)^{15}(1-g)^3}\right]^{\frac{1}{8}}\mathcal{B}_0^3 \times\exp\left[3\omega_0\left(\left(\frac{3}{n+2}\right)\left(\frac{18-15g}{8g\mu(1-n_s)}\right)\right)^{\frac{5g+2}{8g}}\right] \times\left[\left(\frac{3}{n+2}\right)\left(\frac{18-15g}{8g\mu(1-n_s)}\right)\right]^{\frac{g+2}{8g}}. \quad (30)$$

The left graph of Fig. 2 shows that the anisotropic model is incompatible with the WMAP7 data for all the three choices of the dissipation factor. With the help of fine-tuning of the parameters g and μ, we are able to find the range $R < 0.22$ in which $n_s = 0.96$ lies for $\eta_0 = 0.25,\ 1,\ 4$. The compatible

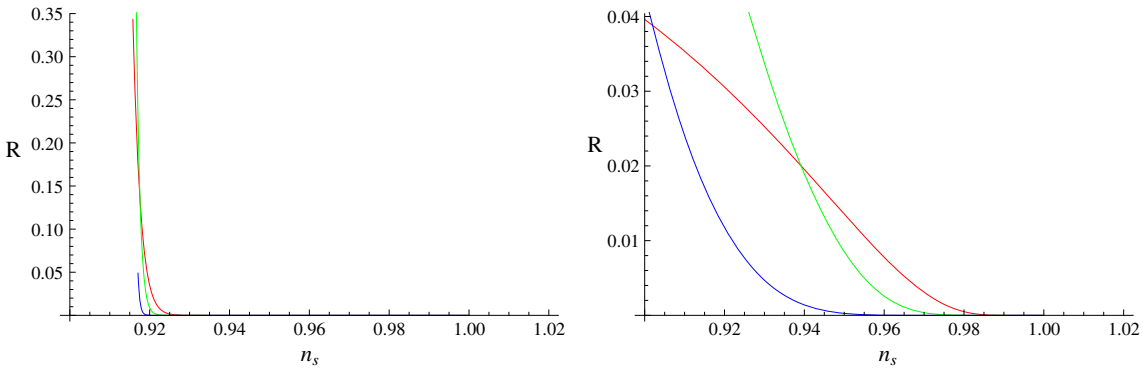

Fig. 2 The *left graph* of scalar–tensor ratio versus n_s for $\mu = 1,\ C_\gamma = 70,\ g = \frac{1}{2},\ \mathcal{B}_0 \propto C_\gamma^{-\frac{1}{12}},\ n \approx 0.5,\ \eta_0 = 0.25$ (*blue*), 1 (*green*), 4 (*red*). The *right graph* is plotted for $\mu = 5,\ g = 0.95$

behavior of the tensor–scalar ratio with the spectral index is shown in the right graph.

3.1.2 Case 2: $\eta = \eta_1 = constant$

Now, we calculate all the above parameters by taking the constant dissipation factor. When η is constant, $\mathcal{B}$ and H_2 take the following form:

$$\mathcal{B} = \mathcal{B}_0 + \omega_1 t^{\frac{2g-1}{2}}, \quad H_2 = \mu g \left(\frac{\mathcal{B}-\mathcal{B}_0}{\omega_1}\right)^{\frac{2(g-1)}{2g-1}}, \tag{31}$$

with $\omega_1 = \left[\frac{8(1+2n)}{\eta_1(2g-1)^2}(1-g)(\mu g)^2\right]^{\frac{1}{2}}$. The corresponding slow-roll parameters are

$$\epsilon = \left(\frac{3}{n+2}\right)\frac{1-g}{\mu g}\left(\frac{\mathcal{B}-\mathcal{B}_0}{\omega_1}\right)^{\frac{2g}{1-2g}},$$
$$\lambda = \left(\frac{3}{n+2}\right)\frac{2-g}{\mu g}\left(\frac{\mathcal{B}-\mathcal{B}_0}{\omega_1}\right)^{\frac{2g}{1-2g}}. \tag{32}$$

In this case, the relationship between ρ_γ and ρ_v becomes

$$\rho_\gamma = \frac{9(1+2n)}{2(n+2)}(\mu g)(1-g)\left(\frac{\mathcal{B}-\mathcal{B}_0}{\omega_1}\right)^{\frac{4-2g}{1-2g}}.$$

The number of e-folds between $\mathcal{B}$ and $\mathcal{B}_1$ is calculated as

$$N = \left(\frac{m+2}{3}\right)\mu\left[\left(\frac{\mathcal{B}-\mathcal{B}_0}{\omega_1}\right)^{\frac{2g}{2g-1}} - \left(\frac{\mathcal{B}_1-\mathcal{B}_0}{\omega_1}\right)^{\frac{2g}{2g-1}}\right], \tag{33}$$

where

$$\mathcal{B}_1 = \mathcal{B}_0 + \omega_1\left[\frac{3(1-g)}{(n+2)\mu g}\right]^{\frac{5g+2}{8g}}.$$

The scalar field in terms of e-folds is given as

$$\mathcal{B} = \mathcal{B}_0 + \omega_1\left[\left(\frac{3}{n+2}\right)\left(\frac{N}{\mu}+\frac{1-g}{g\mu}\right)\right]^{\frac{2g-1}{2g}}. \tag{34}$$

The corresponding scalar power spectrum and spectral index are

$$\Delta_R^2(k) = \left[\left(\frac{3}{2C_\gamma}\right)^{\frac{1}{2}}\frac{(n+2)^{\frac{9}{2}}\eta_1^3(\mu g)^{\frac{3}{2}}}{972(4\pi)^3(1+2n)^{\frac{3}{2}}(1-g)^{\frac{3}{2}}}\right]^{\frac{1}{2}} \times\left[\left(\frac{3}{n+2}\right)\left(\frac{N}{\mu}+\frac{1-g}{g\mu}\right)\right]^{\frac{3}{4}},$$
$$n_s = 1-\left(\frac{9}{4\mu(n+2)}\right)\left[\left(\frac{3}{n+2}\right)\left(\frac{N}{\mu}+\frac{1-g}{g\mu}\right)\right]^{-1}. \tag{35}$$

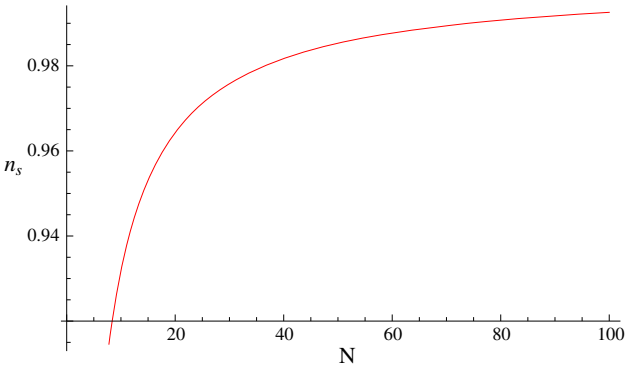

Fig. 3 The graph of n_s versus number of e-folds

The graphical behavior of the spectral index against the number of e-folds is shown in Fig. 3. The corresponding number N of $n_s = 0.96$ decreases as compared to the previous case, in which η is a function of $\mathcal{B}$. In this case, the model remains consistent with WMAP7 observations. Similarly, Δ_T^2 and n_T can be written as

$$\Delta_T^2 = \frac{2}{9\pi^2}(n+2)^2(\mu g)^2\left[\left(\frac{3}{n+2}\right)\left(\frac{N}{\mu}+\frac{1-g}{g\mu}\right)\right]^{\frac{2(g-1)}{g}},$$
$$n_T = -\frac{6(1-g)}{\mu g(m+2)}\left[\left(\frac{3}{n+2}\right)\left(\frac{N}{\mu}+\frac{1-g}{g\mu}\right)\right]^{-1}. \tag{36}$$

The tensor–scalar ratio can be found as

$$R = \left[\frac{48(4\pi)^3(1+2n)^{\frac{3}{2}}(\mu g)^{\frac{5}{2}}(1-g)^{\frac{3}{2}}(2C_\gamma)^{\frac{1}{2}}}{\pi^4\eta_1^3 3^{\frac{1}{2}}(n+2)^{\frac{1}{2}}}\right]^{\frac{1}{2}} \times\left[\left(\frac{3}{n+2}\right)\left(\frac{N}{\mu}+\frac{1-g}{g\mu}\right)\right]^{\frac{5g-8}{4g}},$$
$$= \left[\frac{48(4\pi)^3(1+2n)^{\frac{3}{2}}(\mu g)^{\frac{5}{2}}(1-f)^{\frac{3}{2}}(2C_\gamma)^{\frac{1}{2}}}{\pi^4\eta_1^3 3^{\frac{1}{2}}(n+2)^{\frac{1}{2}}}\right]^{\frac{1}{2}} \times\left[\frac{4\mu(n+2)}{9}(1-n_s)\right]^{\frac{8-5g}{4g}}. \tag{37}$$

Figure 4 shows the agreement of the considered model with WMAP data as the value of observational interest of n_s lies in the region $R < 0.22$.

3.2 Logamediate inflation

Here we evaluate the above-mentioned parameters in the context of logamediate inflation to study the dynamics of warm vector inflation. In this scenario, the scale factor has the specific form [45]

$$b(t) = b_0\exp(\mu[\ln t]^\psi), \quad \psi > 1, \ \mu > 0. \tag{38}$$

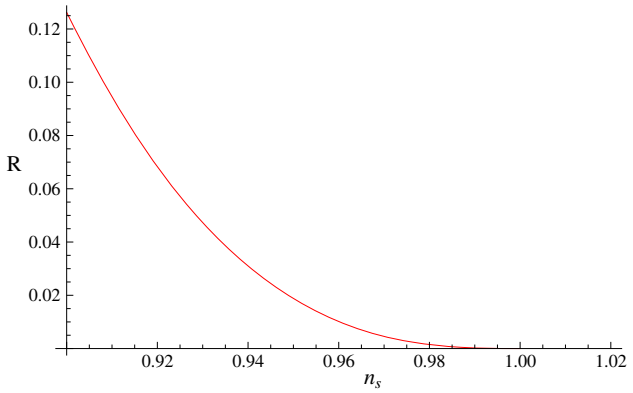

Fig. 4 The graph of the scalar–tensor ratio versus n_s for $\mu = 1$, $C_\gamma = 70$, $g = \frac{1}{2}$, $n \approx 0.5$, $\eta_1 \propto C_\gamma^{\frac{1}{6}}$

Thus the number of e-folds is

$$N = \frac{(n+2)}{3}\mu([\ln t]^\psi - [\ln t_1]^\psi). \tag{39}$$

3.2.1 Case 1: $\eta = \eta_0 \frac{T_\gamma^3}{\mathcal{B}^2}$

In this case, the scalar field and the directional Hubble parameter are

$$\mathcal{B} = \mathcal{B}_0 \exp(\omega_2 \Gamma(t)), \tag{40}$$

$$H_2 = \mu\psi \left(\ln\left[\Gamma^{-1}\left(\frac{\ln\mathcal{B} - \ln\mathcal{B}_0}{\omega_2}\right)\right]\right)^{2(\psi-1)} \times \left[\Gamma^{-1}\left(\frac{\ln\mathcal{B} - \ln\mathcal{B}_0}{\omega_2}\right)\right]^{-2}, \tag{41}$$

where $\omega_2 = \left[\frac{2(2C_\gamma)^{\frac{3}{4}}(\mu\psi)^{\frac{5}{4}}(n+2)^{\frac{3}{4}}(1+2n)^{\frac{1}{4}}}{3^{\frac{7}{4}}\eta_0}\right]^{\frac{1}{2}}$ and $\Gamma(t) = \gamma[\frac{5\psi+3}{8}, \frac{\ln t}{4}]$ is the incomplete gamma function. The potential term is expressed in terms of $\mathcal{B}$ using Eqs. (9) and (40) as

$$V = \frac{2(1+2n)}{3}(\mu\psi)^2 \left(\ln\left[\Gamma^{-1}\left(\frac{\ln\mathcal{B} - \ln\mathcal{B}_0}{\omega_2}\right)\right]\right)^{2(\psi-1)} \times \left[\Gamma^{-1}\left(\frac{\ln\mathcal{B} - \ln\mathcal{B}_0}{\omega_2}\right)\right]^{-2}. \tag{42}$$

The slow-roll parameters can be described as

$$\epsilon = \frac{3}{(n+2)\mu\psi}\left(\ln\left[\Gamma^{-1}\left(\frac{\ln\mathcal{B} - \ln\mathcal{B}_0}{\omega_2}\right)\right]\right)^{2(\psi-1)},$$
$$\lambda = \frac{6}{(n+2)\mu\psi}\left(\ln\left[\Gamma^{-1}\left(\frac{\ln\mathcal{B} - \ln\mathcal{B}_0}{\omega_2}\right)\right]\right)^{2(\psi-1)}. \tag{43}$$

The corresponding energy density of radiation is

$$\rho_\gamma = \frac{9(1+2n)}{2(m+2)}(\mu\psi)\left(\ln\left[\Gamma^{-1}\left(\frac{\ln\mathcal{B} - \ln\mathcal{B}_0}{\omega_2}\right)\right]\right)^{6(\psi-1)} \times \left(\Gamma^{-1}\left(\frac{\ln\mathcal{B} - \ln\mathcal{B}_0}{\omega_2}\right]\right)^{-4}.$$

The number of e-folds between two fields is given as

$$N = \left(\frac{n+2}{3}\right)\mu\left[\left(\ln\left[\Gamma^{-1}\left(\frac{\ln\mathcal{B} - \ln\mathcal{B}_0}{\omega_2}\right)\right]\right)^{\psi} - \left(\frac{(n+2)}{3}\mu\psi\right)^{\frac{\psi}{1-\psi}}\right]. \tag{44}$$

The second equality in the above equation is obtained by using the value of $\mathcal{B}_1$ and putting $\epsilon = 1$. Equation (40) can be rewritten in terms of e-folds as

$$\mathcal{B} = \mathcal{B}_0 \exp\left[\omega_2\Gamma \exp\left[\left(\frac{3}{n+2}\right)\frac{N}{\mu} + \left(\frac{3}{n+2}\mu\psi\right)^{\frac{\psi}{1-\psi}}\right]^{\frac{1}{\psi}}\right]. \tag{45}$$

The corresponding perturbed parameters $\Delta_R^2(k)$ and $\Delta_T^2(k)$ are

$$\Delta_R^2(k) = \left(\frac{\eta_0^3}{(4\pi)^3}\right)^{\frac{1}{2}}\left[\frac{3^{11}(m+2)^9(\mu\psi)^{15}(1+2n)^3}{(2C_\gamma)^{11}}\right]^{\frac{1}{8}}\mathcal{B}_0^{-3} \times \exp\left[-3\omega_2\Gamma\exp\left[\left(\frac{3}{n+2}\right)\frac{N}{\mu} + \left(\frac{3}{n+2}(\mu\psi)\right)^{\frac{\psi}{1-\psi}}\right]^{\frac{1}{\psi}}\right] \times \exp\left[\frac{-15}{8}\left(\exp\left[\left(\frac{3}{n+2}\right)\frac{N}{\mu} + \left(\frac{3}{n+2}(\mu\psi)\right)^{\frac{\psi}{1-\psi}}\right]^{\frac{1}{\psi}}\right)\right] \times \left[\left(\frac{3}{n+2}\right)\frac{N}{\mu} + \left(\frac{3}{n+2}(\mu\psi)\right)^{\frac{\psi}{1-\psi}}\right]^{\frac{15(\psi-1)}{8\psi}}, \tag{46}$$

$$\Delta_T^2 = \frac{2}{9\pi^2}(m+2)^2(\mu\psi)^2\left[\left(\frac{3}{n+2}\right)\frac{N}{\mu} + \left(\frac{3}{n+2}(\mu\psi)\right)^{\frac{\psi}{1-\psi}}\right]^{\frac{2(\psi-1)}{\psi}} \times \exp\left[-2\left(\left(\frac{3}{n+2}\right)\frac{N}{\mu} + \left(\frac{3}{n+2}(\mu\psi)\right)^{\frac{\psi}{1-\psi}}\right)^{\frac{1}{\psi}}\right]. \tag{47}$$

The corresponding spectral indices are

$$n_s - 1 = \frac{15(1-\psi)}{8\mu\psi}\left(\frac{3}{n+2}\right)\left[\left(\frac{3}{n+2}\right)\frac{N}{\mu} + \left(\frac{3}{n+2}(\mu\psi)\right)^{\frac{\psi}{1-\psi}}\right]^{-1}, \tag{48}$$

$$n_T = -\frac{6}{(n+2)\mu\psi}\left[\left(\frac{3}{n+2}\right)\frac{N}{\mu} + \left(\frac{3}{n+2}(\mu\psi)\right)^{\frac{\psi}{1-\psi}}\right]^{1-\psi}.$$

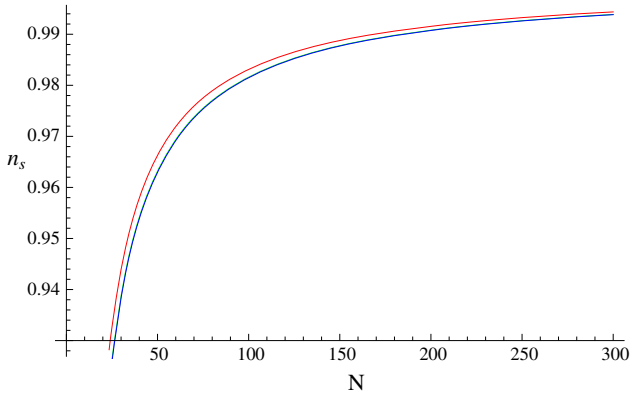

Fig. 5 The graph of n_s versus number of e-folds for $\mu = 1,\ \psi = 10$ (*red*), 50 (*blue*), $n \approx 0.5$ in logamediate scenario

Figure 5 indicates the behavior of n_s against N for $\psi = 10,\ 50$. The number of e-folds decreases as ψ increases. Here the allowed value of the parameter $n_s = 0.96$ lies in the range $N \approx 50$. Finally, we obtain the following observational parameter of interest as a function of the spectral index:

$$R = \left(\frac{4(4\pi)^3}{81\pi^4\eta_0^3}\right)^{\frac{1}{2}} \left[\frac{(2C_\gamma)^{11}(n+2)^7(\mu\psi)}{3^{11}(1+2n)^3}\right]^{\frac{1}{8}} \times \mathcal{B}_0^3 \left[\left(\frac{3}{n+2}\right)\frac{15(\psi-1)}{8\mu\psi(1-n_s)}\right]^{\frac{1}{\psi}} \times \exp\left[3\omega_2\Gamma \exp\left[\left(\frac{3}{n+2}\right)\frac{15(\psi-1)}{8\mu\psi(1-n_s)}\right]^{\frac{1}{\psi}}\right] \times \exp\left[-\frac{1}{8}\left[\left(\frac{3}{n+2}\right)\frac{15(\psi-1)}{8\mu\psi(1-n_s)}\right]^{\frac{1}{\psi}}\right]. \quad (49)$$

We see from Fig. 6 the consistency of the model with the observational data for specific values of η_0. The ratio R decreases as ψ increases.

3.3 Case 2: $\eta = \eta_1$

For this case, the scalar field and the directional Hubble parameter are

$$\mathcal{B} = \mathcal{B}_0 + \omega_3\Gamma(t), \quad H_2 = \frac{\mu\psi\left(\ln\left[\Gamma^{-1}\left(\frac{\mathcal{B}-\mathcal{B}_0}{\omega_3}\right)\right]\right)^{(\psi-1)}}{\Gamma^{-1}\left(\frac{\mathcal{B}-\mathcal{B}_0}{\omega_3}\right)}, \quad (50)$$

where $\omega_3 = \left[\frac{2(1+2n)(\mu\psi)^2}{\eta_1}\right]^{\frac{1}{2}} \frac{(\psi-1)!}{2^{\psi-1}}$ and $\Gamma(t) = \gamma[\psi, \frac{\ln t}{2}]$. In this case, V is transformed into

$$V = \frac{2(1+2n)}{3}\left[\frac{(\mu\psi)\left(\ln\left[\Gamma^{-1}\left(\frac{\mathcal{B}-\mathcal{B}_0}{\omega_3}\right)\right]\right)^{(\psi-1)}}{\Gamma^{-1}\left(\frac{\mathcal{B}-\mathcal{B}_0}{\omega_3}\right)}\right]^2.$$

The parameters ϵ and λ take the following form:

$$\epsilon = \frac{3\left(\ln\left[\Gamma^{-1}\left(\frac{\mathcal{B}-\mathcal{B}_0}{\omega_3}\right)\right]\right)^{1-\psi}}{(n+2)(\mu\psi)}, \quad \lambda = \frac{6\left(\ln\left[\Gamma^{-1}\left(\frac{\mathcal{B}-\mathcal{B}_0}{\omega_3}\right)\right]\right)^{1-\psi}}{(n+2)(\mu\psi)}. \quad (51)$$

The number of e-folds becomes

$$N = \left(\frac{n+2}{3}\right)\mu\left[\left(\ln\left[\Gamma^{-1}\left(\frac{\mathcal{B}-\mathcal{B}_0}{\omega_3}\right)\right]\right)^{\psi} - \left[\frac{n+2}{3}(\mu\psi)\right]^{\frac{\psi}{1-\psi}}\right]. \quad (52)$$

The scalar field is

$$\mathcal{B} = \mathcal{B}_0 + \omega_3\Gamma \exp\left[\left(\frac{3}{n+2}\right)\frac{N}{\mu} + \left(\frac{n+2}{3}(\mu\psi)\right)^{\frac{\psi}{1-\psi}}\right]^{\frac{1}{\psi}}. \quad (53)$$

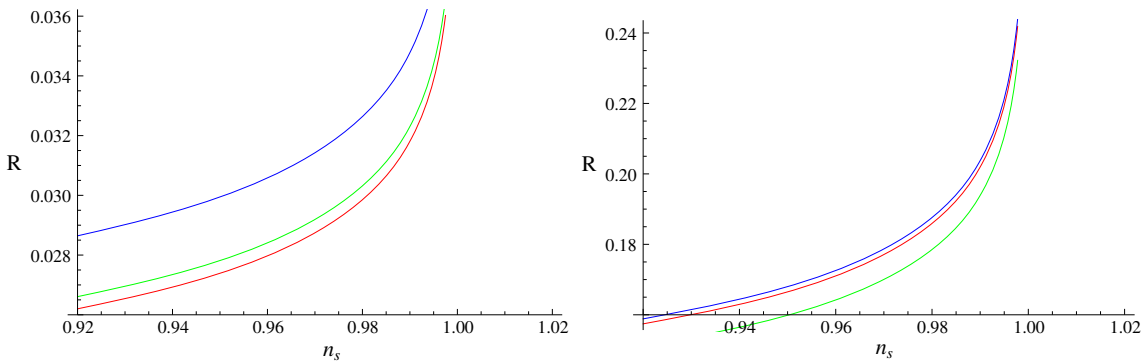

Fig. 6 The *left graph* of scalar–tensor ratio versus n_s for $\mu = 1,\ C_\gamma = 70,\ f = \frac{1}{2},\ n \approx 0.5,\ \mathcal{B}_0 \propto C_\gamma^{-\frac{1}{12}},\ \psi = 10,\ \eta_0 = 0.25$ (*blue*), 1 (*green*), 4 (*red*). The *right graph* is plotted for $\psi = 50$

The power spectra in scalar and tensor forms can be found as

$$\Delta_R^2(k) = \left(\frac{\eta_1^3(n+2)^{\frac{9}{2}}3^{\frac{1}{2}}(\mu\psi)^{\frac{3}{2}}}{972(1+2n)^{\frac{3}{2}}(4\pi)^3(2C_\gamma)^{\frac{1}{2}}}\right)^{\frac{1}{2}}\left[\left(\frac{3}{n+2}\right)\frac{N}{\mu} + \left(\frac{n+2}{3}(\mu\psi)\right)^{\frac{\psi}{1-\psi}}\right]^{\frac{3(\psi-1)}{4\psi}},$$

$$\Delta_T^2(k) = \frac{2(1+2n)}{3\pi^2}(\mu\psi)^2\left[\left(\frac{3}{n+2}\right)\frac{N}{\mu} + \left(\frac{3}{n+2}(\mu\psi)\right)^{\frac{\psi}{1-\psi}}\right]^{\frac{2(\psi-1)}{\psi}} \times \exp\left[-2\left(\left(\frac{3}{n+2}\right)\frac{N}{\mu}+\left(\frac{3}{n+2}(\mu\psi)\right)^{\frac{\psi}{1-\psi}}\right)^{\frac{1}{\psi}}\right]. \quad (54)$$

The terms n_s and n_T related to the above equations become

$$n_s - 1 = \frac{9(1-\psi)}{4\mu\psi(n+2)}\left[\left(\frac{3}{n+2}\right)\frac{N}{\mu}+\left(\frac{n+2}{3}(\mu\psi)\right)^{\frac{\psi}{1-\psi}}\right]^{-1},$$

$$n_T = -\frac{6}{(n+2)\mu\psi}\left[\left(\frac{3}{n+2}\right)\frac{N}{\mu}+\left(\frac{n+2}{3}(\mu\psi)\right)^{\frac{\psi}{1-\psi}}\right]^{\frac{1-\psi}{\psi}}. \quad (55)$$

Figure 7 shows a similar behavior to behavior for the large values of ψ giving small values of the N. The value $N \approx 20$ coincides with $n_s = 0.96$ and verifies the compatibility of this case with the observational data. The curves for $\psi = 50$ and $\psi = 70$ overlap in the allowed range. Consequently, R can be represented as

$$R = \left(\frac{3888(1+2n)^{\frac{7}{2}}(4\pi)^3(2C_\gamma)^{\frac{1}{2}}(\mu\psi)^{\frac{5}{2}}}{81\pi^4\eta_1^3(n+2)^{\frac{9}{2}}3^{\frac{5}{2}}}\right)^{\frac{1}{2}} \times\left[\left(\frac{3}{n+2}\right)\frac{3(\psi-1)}{4\mu\psi(1-n_s)}\right]^{\frac{5(\psi-1)}{4\psi}} \times \exp\left[-2\left(\left(\frac{3}{n+2}\right)\frac{3(\psi-1)}{4\mu\psi(1-n_s)}\right)^{\frac{1}{\psi}}\right]. \quad (56)$$

Figure 8 verifies the compatibility of the anisotropic BI model of the universe in the constant logamediate inflation regime with WMAP7 data.

4 Concluding remarks

It is well known that inflation due to scalar fields is compatible with a completely isotropic universe. In this paper, we assume vector field inflation, which can provide the isotropic (by orthogonal triplet vector fields) as well as anisotropic universe (with randomly oriented N vector fields). The anisotropic fields can be achieved in two ways, i.e., by applying initial conditions on the potential and fine-tuning of the inflationary time period. The anisotropy is of the order $1/\sqrt{N}$ at the end of inflation. We have investigated the role of warm vector inflation in the framework of the LRS BI model of the universe. A triplet of mutually orthogonal vectors is introduced to remove the off-diagonal terms from the components of the energy-momentum tensor as the considered model is symmetric. We construct the field equations and conservation equations in the slow-roll approximation using a specific form of the dissipation coefficient. We have assumed the dissipation of the inflaton density into radiation density ($\eta > 0$).

The slow-roll parameters (ϵ, λ) are presented in the context of anisotropic warm vector inflation. Using these parameters and applying the strong dissipative regime, we have calculated the more general conditions for the starting and ending of the inflationary era (13). In warm inflation, thermal fluctuations are produced instead of quantum fluctuations, which are characterized by the power spectra $(\Delta_R^2(k), \Delta_T^2(k))$ and spectral indices (n_S, n_T). We have eval-

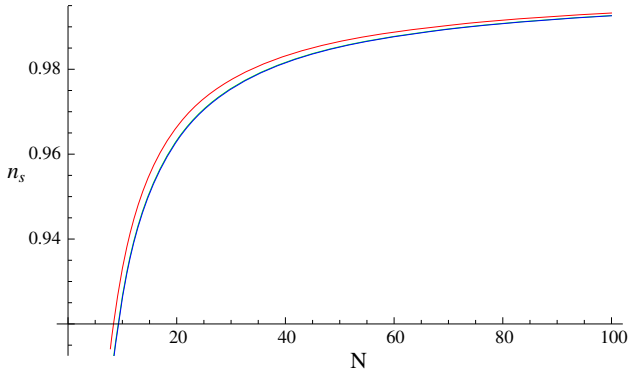

Fig. 7 The graph of n_s versus number of e-folds for $\mu = 1$, $\psi = 10$ (*red*), 50 (*green*), 70 (*blue*), $n \approx 0.5$

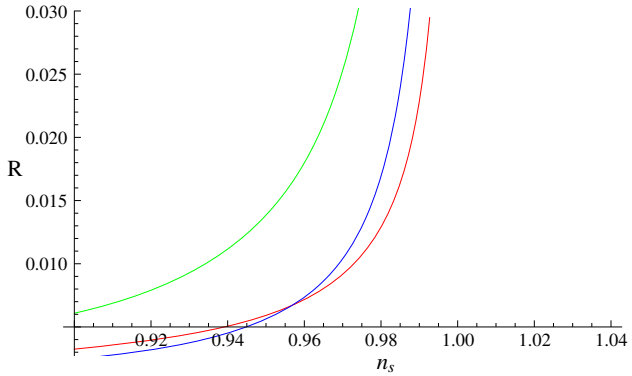

Fig. 8 The graph of scalar–tensor ratio versus n_s for $\mu = 1$, $C_\gamma = 70$, $\psi = 10$ (*red*), 50 (*green*), 70 (*blue*), $n \approx 0.5$, $\eta_1 \propto C_\gamma^{\frac{1}{6}}$

uated all these perturbed parameters under slow-roll conditions and finally an important parameter, i.e., the tensor–scalar ratio, which is constrained by WMAP7 observations.

We have developed our model into intermediate and logamediate models as they represent exact cosmological solutions. Each era is discussed for two possible choices of η, i.e., it is a function of scalar field or some positive constant. The directional Hubble parameter, and slow-roll as well as perturbation parameters are calculated in these frameworks of inflation for an anisotropic universe. According to the observations of WMAP7, the best fit values of these parameters $(\Delta_R^2(k), n_S, R)$ have been calculated with a higher degree of accuracy. We have checked the physical compatibility of our model with the results of WMAP7, i.e., the standard value $n_S = 0.96$ must be found in the region $R < 0.22$. The behavior of these parameters is checked through graphs of N and R versus n_S in each case.

During the intermediate scenario with variable η, we have seen that $n_S = 0.96$ corresponds to $N = 50$. The left R–n_S trajectories in Fig. 2 show the inconsistency of the model with WMAP7 for $\mu = 1,\ C_\gamma = 70,\ g = \frac{1}{2},\ \mathcal{B}_0 \propto C_\gamma^{-\frac{1}{12}},\ n \approx 0.5,\ \eta_0 = 0.25,\ 1,\ 4$. The method of fine-tuning helps one to find the allowed range and hence $n_S = 0.96$ is located in the region $R < 0.22$ for $\mu = 5,\ g = \frac{1}{2},\ \mathcal{B}_0 \propto C_\gamma^{-\frac{1}{12}},\ n \approx 0.5,\ \eta_0 = 0.25,\ 1,\ 4$. The isotropic universe [51] for this case is compatible with WMAP7 only for $\eta_0 = 1$, keeping the same rest of the parameters the same. For constant η, the model remains compatible with the observational data. Hence the anisotropic model of the universe is compatible with the WMAP7 data during variable and constant intermediate inflation. Figures 5, 6, 7, and 8 indicate the compatibility of the variable as well as constant logamediate inflationary scenario in the framework of anisotropic universe with the WMAP7 data. We would like to mention here that this model is consistent for all chosen values of ψ and η_0, while the isotropic universe for a variable dissipation factor is compatible only for $\eta_0 = 1$. We have also observed that the compatibility of the model is disturbed for large values of the anisotropic parameter (n). It is interesting that all the results reduce to the isotropic universe (FRW) for $n = 1$. Anisotropic warm inflation can be discussed in the intermediate and logamediate scenarios using gauge fields.

References

1. S. Perlmutter et al., Astron. Soc. **29**, 1351 (1997)
2. S. Perlmutter et al., Nature **391**, 51 (1998)
3. A.G. Riess et al., Astron. J. **116**, 1009 (1998)
4. C.L. Bennett et al., Astrophys. J. Suppl. **148**, 1 (2003)
5. P.J.E. Peebles, B. Ratra, Rev. Mod. Phys. **75**, 559 (2003)
6. M. Tegmark et al., Phys. Rev. D **69**, 03501 (2004)
7. D.N. Spergel et al., Astrophys. J. Suppl. **170**, 377 (2007)
8. F. Darabi. arXiv:1107.3307
9. B. Ratra, P.J.E. Peebles, Phys. Rev. D **37**, 3406 (1998)
10. T. Chiba, T. Okabe, M. Yamaguchi, Phys. Rev. D **62**, 023511 (2000)
11. A. Sen, J. High Energy Phys. **48**, 204 (2002)
12. T. Padmanabhan, Phys. Rev. D **66**, 021301 (2002)
13. Z.K. Guo et al., Phys. Lett. B **608**, 177 (2005)
14. T. Padmanabhan, Gen. Relativ. Gravit. **40**, 529 (2008)
15. V. Gorini, A. Kamenshchik, U. Moschella, Phys. Rev. D **67**, 063509 (2003)
16. B. Wang, Y.G. Gong, E. Abdalla, Phys. Lett. B **624**, 141 (2005)
17. B. Hu, Y. Ling, Phys. Rev. D **73**, 123510 (2006)
18. M.R. Setare, J. Cosmol. Astrophys. **0701**, 023 (2007)
19. A.A. Starobinsky, Phys. Lett. B **91**, 99 (1980)
20. A. Guth, Phys. Rev. D **23**, 347 (1981)
21. A. Albrecht, P.J. Steinhardt, Phys. Rev. Lett. **48**, 1220 (1982)
22. A.D. Linde, Phys. Lett. B **108**, 389 (1982)
23. B. Gold, et al. arXiv:1001.4555
24. E. Komatsu et al., Astrophys. J. Suppl. **192**, 18 (2011)
25. D. Larson et al., Astrophys. J. Suppl. **192**, 16 (2011)
26. A. Golovnev, V. Mukhanov, V. Vanchurin, J. Cosmol. Astropart. Phys. **0806**, 009 (2008)
27. B. Himmetoglu, C.R. Contaldi, M. Peloso, Phys. Rev. D **80**, 123530 (2009)
28. J.M. Bardeen, P.J. Steinhardt, M.S. Turner, Phys. Rev. D **28**, 679 (1983)
29. A. Linde, Phys. Lett. B **129**, 177 (1983)
30. E.W. Kolb, M.S. Turner, *The Early Universe* (Addison-Wesley, New York, 1990)
31. B.A. Bassett, S. Tsujikawa, D. Wands, Rev. Mod. Phys. **78**, 537 (2006)
32. A. Berera, Phys. Rev. Lett. **75**, 3218 (1995)
33. A. Berera, Phys. Rev. D **55**, 3346 (1997)
34. I.G. Moss, Phys. Lett. B **154**, 120 (1985)
35. A. Berera, Nucl. Phys. B **585**, 666 (2000)
36. L.M.H. Hall, I.G. Moss, A. Berera, Phys. Rev. D **69**, 083525 (2004)
37. A.K. Sanyal, Phys. Lett. B **645**, 1 (2007)
38. T. Koivisto, D.F. Mota, Phys. Lett. B **644**, 104 (2007)
39. T. Koivisto, D.F. Mota, Phys. Rev. D **75**, 023518 (2007)
40. S. Mignemi, N. Stewart, Phys. Rev. D **47**, 5259 (1993)
41. S. Nojiri, S.D. Odintsov, M. Sasaki, Phys. Rev. D **71**, 123509 (2005)
42. G. Cognola, E. Elizalde, S. Nojiri, S.D. Odintsov, S. Zerbini, Phys. Rev. D **73**, 084007 (2006)
43. I. Antoniadis, J. Rizos, K. Tamvakis, Nucl. Phys. B **415**, 497 (1994)
44. J. Yokoyama, K. Maeda, Phys. Lett. B **207**, 31 (1988)
45. J.D. Barrow, Class. Quantum Grav. **13**, 2965 (1996)
46. J.D. Barrow, Phys. Rev. D **51**, 2729 (1995)
47. P.G. Ferreira, M. Joyce, Phys. Rev. D **58**, 023503 (1998)
48. J.D. Barrow, N.J. Nunes, Phys. Rev. D **76**, 043501 (2007)
49. M.R. Setare, V. Kamali. arXiv:1308.5674
50. M. Jamil, D. Momeni, M.R. Setare. arXiv:1309.3269
51. M.R. Setare, V. Kamali. arXiv:1309.2452
52. C.B. Collins, Phys. Lett. A **60**, 397 (1977)
53. M. Sharif, M. Zubair, Astrophys. Space Sci. **330**, 399 (2010)
54. C. Armendariz-Picon, J. Cosmol. Astropart. Phys. **07**, 007 (2004)
55. V. Mukhanov, Physical Foundations of Cosmology (Cambridge University Press, Cambridge, 2005)
56. M. Bastero-Gil, A. Berera, R.O. Ramos, J. Cosmol. Astropat. Phys. **1109**, 033 (2011)
57. M. Bastero-Gil, A. Berera, R.O. Ramos, J.G. Rosa, J. Cosmol. Astropart. Phys. **1301**, 016 (2013)

58. J.C. Hwang, H. Noh, Phys. Rev. D **66**, 084009 (2002)
59. A.H. Guth, S.Y. Pi, Phys. Rev. Lett. **49**, 1110 (1982)
60. S.W. Hawking, Phys. Lett. B **115**, 295 (1982)
61. A.A. Starobinsky, Phys. Lett. B **117**, 175 (1982)
62. J.M. Bardeen, P.J. Steinhardt, M.S. Turner, Phys. Rev. D **28**, 679 (1983)
63. K. Freese, J.A. Frieman, A.V. Olinto, Phys. Rev. Lett. **65**, 3233 (1990)